Comparative Study of the Potential Therapeutic Role of each of Platelet- rich plasma, Mesenchymal Stem Cells and Stem Cells Derived Extracellular Vesicles in Treatment of Skin Wound in Adult Male Albino Rat: Histological, Immunohistochemical and Biochemical Study

Medhat Mohamed Morsi [1]; **Hanan Nabih Gadallah**[1]; **Reham Farouk Abd Elaleem Elazab**[1]; **Marwa Mohammed Abdelgwad Soliman** [2]; Ghada Nady Ouais [1&3]

[1] *Anatomy and Embryology Department, Faculty of Medicine, Cairo University, Cairo 11562, Egypt*

[2] *Medical Biochemistry and molecular biology, Faculty of Medicine, Cairo University*

[3] *Anatomy and Embryology Department, Faculty of Medicine, New Giza University, Giza 12211, Egypt*

Corresponding author: Ghada Nady Ouais:
ghada.nady@kasralainy.edu.eg

Abstract

Through scientific literature, wound healing represents an important medical problem. It is a complex biological process. This work might draw attention to the effective and promising role of BM-MSCs, extracellular vesicles and PRP on histological, immunohistochemical and biochemical evaluations of the three regimens on healing of skin wound. This study carried out on 60 albino male rats; a full-thickness skin square wound (1.5x1.5 cm^2) wound was created on the middle of the dorsum of the trunk in the rats. BM-MSCs, extracellular vesicles (exosomes that derived from stem cells) and PRP were injected intradermal into the four corners of the wound. On the 7^{th} and 21^{st} post-operative days, biopsies were taken to be examined under a light microscope at both stages of wound healing, allowing for a sequential evaluation of wound healing. Our work proved that BM-MSCs, extracellular vesicles and PRP showed improvement in regeneration of the epidermis and dermis in all healing process stages. Regarding the inflammation and angiogenesis, the treated groups showed moderate degree of inflammation and neovascularization especially exosomes treated group. Epithelization improved in all treated groups especially the stem cells treated group. Also collagen formation and deposition enhanced in all treated groups especially stem cells and exosomes treated groups. Elasticity of the skin was improved by the three modalities.

Conclusion: The outcomes of this study indicated that applying biocellular products may assist skin wound healing by changing the microenvironment that could contribute to the earliest possible epithelialization of the entire wound. Moreover, exosomes therapy has an optimistic outlook due to their outstanding results, ease of use, lower cost than PRP, and being non-cellular compared to stem cells.

Keywords: Wound healing, Skin wound, BM-MSCs, exosomes, PRP.

Introduction

The skin wounds are frequently occur as acute or chronic wounds, for example, diabetic skin ulcerations or burn wounds which lead to physical and mental suffering in the affected individuals and big financial burdens at the familial and societal levels**(1)**

The healing process consists of four phases; hemostasis, inflammation, cell proliferation, and matrix remodeling. The phases of wound healing are overlapping

(2). Stem cell therapy is one of the most promising treatments for wound healing, as it has the potential to restore damaged tissues due to its special capacity for self-renewal and differentiation **(3).** The mesenchymal stem cells (MSCs) have a significant promise for regenerative medicine due to convenient isolation, low immunogenicity, the ability to differentiate, and create a favorable environment for tissue regeneration **(4&5)**.Clinical investigations using BM-MSCs showed positive outcomes without any evident harm in participants **(6).**

PRP is a plasma preparation that contains an autologous concentration of platelets above background levels. Multiple growth and differentiation agents are produced and released, which underlies the PRP's physical characteristics **(7).** PRP gel is frequently utilized to speed up the recovery of chronic cutaneous non-healing wounds **(8).** As it expedites bone production, it is also applied in the field of surgery to cure a number of hard tissue problems **(9).**

Recently, a novel approach known as "cell-free therapy" that employs extracellular vehicles (EVs) produced from cells for tissue restoration has been implemented **(10).** EVs are membrane structures that are released by different cells; they can transport bioactive molecular contents to target cells in wounded tissue, such as proteins, mRNAs, and miRNA sequences **(11).** There is growing evidence that mesenchymal stem/stromal cells (MSCs) create EVs that have therapeutic effects in a variety of disease models **(12).**

Materials and Methods

Chemicals: All are obtained from Biochemistry Department, Kasr Al-Ainy School of medicine and prepared separately as follow**:**

1-Bone marrow- derived mesenchymal stem cells (BM-MSCs) is suspended in distilled, sterile water and each rat was received 1ml of the prepared dose intradermal (1×10^7 cells suspended in 1 ml of PBS)

Preparation, isolation and identification of BM-MSCs in culture:

To separate mononuclear cells (MNCs), rat bone marrow was employed. Phosphate-Buffered Saline (PBS) was used to flush BM cells from the tibia of white albino rat bones. Bone marrow cells was carefully stacked over 15 ml Ficoll-Paque (Gibco-Invitrogen, Grand Island, NY), then they were centrifuged for 35 min. at 400xg rpm. The isolated BM-MSCs were cultured and propagated on 25 ml culture flasks in Roswell Park Memorial Institute (RPMI)-1640 medium supplemented with 10% Foetal Bovine Serum (FBS), 0.5% penicillin, and streptomycin, and incubated at 37°C and 5% CO2 until reaching 80-90% confluence within 7 days. At 3, 7 and 14 days, the morphology of cultured MSCs was examined under an electron microscope (EM) to determine their characteristics. Additionally, CD45- and CD90+ positivity specific to MSCs were assessed **(Fig.1 A, B, C)**.

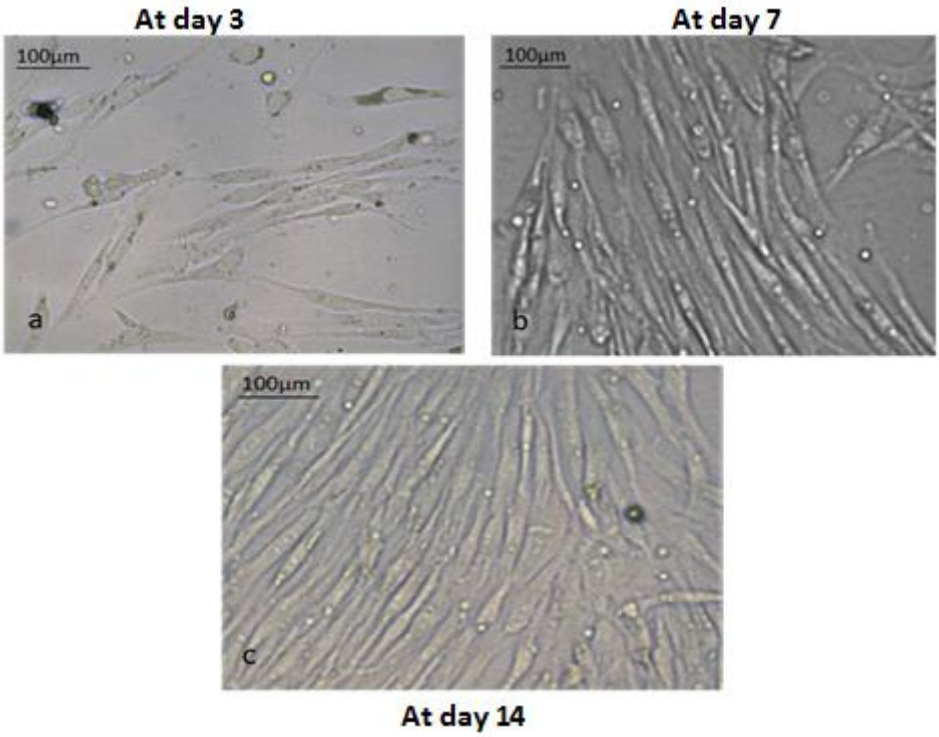

Fig.1: Micrographs showing Mesenchymal stem cells at day 3, 7 and 14

2-Exosomes (EVs) are suspended in distilled, sterile water and each rat received 1ml of the prepared dose intradermal (200 µg extracellular vesicles derived from stem cells suspended in 1 ml PBS).

Preparation and identification of EVs derived from BM-MSCs (13):

Supernatants of MSCs were used to extract EVs. To obtain EVs, after centrifugation at 10,000 g for 20 minutes to remove debris, cell-free supernatants were centrifuged for one hour at 4°C, washed in medium 199 containing N-2-Hydroxy Ethyl Piperazine-N'-2-Ethane Sulfonic acid (HEPES) 25 mM (Sigma) and submitted to a second ultracentrifugation in the same conditions. CD63 and CD81 western blots and electron microscope (EM) examinations were used for describing EVs.

Western blot for Characterization of EVs:

The antibodies used were polyclonal sheep IgG anti-rabbit CD81 (Biolegend, Cat N: 0349509) and monoclonal antibody anti-rattus CD63 (Novus Biological, Cat N: NBP2-36567). Protein isolated from isolated MSCs and EVs using RIPA buffer. The isolated protein (20 gram) was added and separated using SDS-PAGE. Polyclonal monoclonal antibody was added to one membrane that containing the specimen sample then incubated at 4 °C. A competent secondary antibody was incubated at room temperature for two hours. Densitometric analysis of the immunoblots was carried out using image analysis software to quantify the quantities of CD81 against the housekeeping protein β-actin. After being washed, EVs were fixed for 2 hours with 2.5% glutaraldehyde before being ultra-centrifuged. A formvar/carbon-coated grid was loaded with 20uL of EVs, which were then negatively stained with 3% aqueous phosphor-tungstic acid for one minute and then viewed by EM (HITACHI, H-7650, Japan). EM demonstrated the spheroid morphology and verified the size of pure EVs **(Fig. 2).**

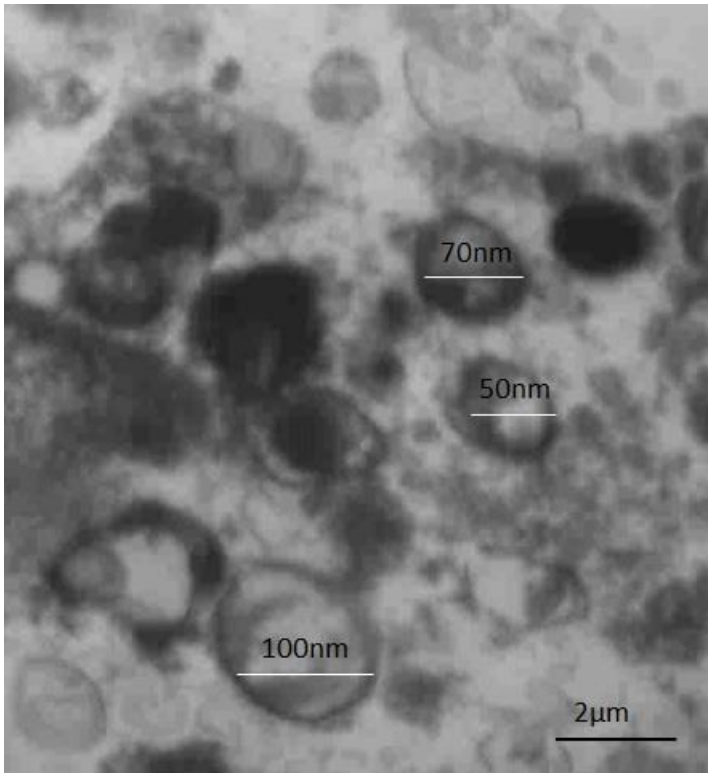

Fig.2: Micrograph showing Exosomes morphology and size.

3-PRP is prepared in a solution form and each rat received 1ml of the prepared dose intradermal ($80x10^4$ platelets/µl).

Preparation of PRP (14):

A sample of 10 ml blood was drawn from each rat (from retro-orbital vein) into vacuum tubes containing 10% sodium citrate. A double-centrifugation procedure was used to prepare the PRP. **First centrifugation:** Using a laboratory centrifuge (Beckman Centrifuge, CA, USA), the components of the blood cell were separated. The blood cell component (BCC) and Serum component (SEC) were obtained after the first centrifugation. **Second centrifugation:** A mark was made 6 mm below the line that separated the BCC from the SEC. All material over this point is pipetted and transferred to another 5 ml vacuum tube without anticoagulant in order to enhance the total amount of platelets collected for the second centrifugation. The material was then centrifuged again for 15 minutes resulting in two components: SEC and PRP. The PRP and SEC were split apart.

Animals

The present study conducted on sixty adult male albino rats weighing 180-200 grams. Rats were provided by the Animal House, Faculty of Medicine, Cairo University, and were cared for throughout the experiment according to the standards of the animal ethics committee **(approval number: CU III F 47 21).** Rats were kept in cages with periodic light and dark cycles, access to food, and a comfortable temperature. To prevent infection or additional wound injury, the rats were housed individually. Every day, the state of the wounds was checked to look for any infection or oozing. All Rats in the groups (II, III, IV and V) were undergoing surgical wound, the rats were anesthetized by intraperitoneal injection of 50 mg/kg pentobarbital. Electric razors were used to shave the surgical region, and 70% ethanol was used to clean it. Under typical sterile circumstances, a 1.5x1.5 cm2 square wound was made on the center of the dorsum of the trunk (Fig. 3). A full thickness wound was made by cutting the

epidermal and dermal layers down to the subcutaneous connective tissue **(15).** Rats were randomly divided into five equal groups (twelve in each):

Fig. 3: Micrographs showing preparations of the wound at the dorsum of the rats and intradermal injections of the therapies into the corners of the wound**.**

Experimental Design

Group I (Control): Rats did not have wound, nor received treatment sacrificed at the 7^{th} day.

Group II: (operated control: skin wound with no treatment) rats equitably divided into two subgroups (six in each); **subgroup II a** sacrificed at the 7^{th} day while **subgroup II b** sacrificed at the 21^{st} day **(16)**.

Group III (Skin wound treated with MSCs): The rats were injected once with BM-MSCs at a dosage of 1×10^7 cells per rat suspended in 1 ml of PBS. They were promptly injected intradermal using Short Needle Insulin Syringe in the corners of the surgical skin wound ,then equitably divided into two subgroups (six in each); **subgroup III a** sacrificed at the 7^{th} day while **subgroup III b** sacrificed at the 21^{st} day **(15)**.

Group IV (skin wound treated with exosomes) : The rats were promptly injected with 200 µg extracellular vesicles obtained from stem cells suspended in 1 ml PBS in the edges of the surgical skin wound intradermal, the 3^{rd} day and in the 7^{th} day after the wound induction using short needle insulin syringe ,then equitably divided into two subgroups (six in each); **subgroup IV a** sacrificed at the 7^{th} day while **subgroup IV b** sacrificed at the 21^{st} day **(1)**.

Group V (Skin wound treated with PRP): The rats were injected with PRP as intradermal 1ml of the prepared dose on 4 corners. They will be injected intradermal immediately, the 3^{rd} day and in the 7^{th} day after the wound induction using Short Needle Insulin Syringe, then equitably divided into two subgroups (six in each); **subgroup V a** sacrificed at the 7^{th} day while **subgroup V b** sacrificed at the 21^{st} day **(17).**

Scarification:

The animals were sacrificed by intraperitoneal injection of phenobarbitone sodium (80μg/kg) after light ether inhalation, to avoid chemical injury. Skin samples were taken in full thickness including about 0.5 cm around the healing wound were taken and each specimen was excised equally into two equal halves, one of them preserved in 10% buffered formalin solution and the other half was preserved frozen at -80 c° for the biochemical assessment.

Methods:

1-Histological study:

The skin specimens for histological examination that were taken at 7th day and at the 21st day after wound induction **(18)**. The specimens were flattened, fixed in 10% buffered formalin solution for 24-48 hours, dehydrated in ascending grades of ethanol and embedded in paraffin. Serial sections of 7 μ m thicknesses will be cut and subjected to the following stains: Haematoxylin & Eosin (H&E) stain for histological evaluation **(19),** Masson's trichrome stain for detection of collagen fibers **(20)** and Orcein stain for detection of elastic fibers **(21).**

2-Immunohistochemical study:

Immunohistochemical stain was performed for the demonstration of Proliferating Cell Nuclear Antigen (PCNA) in the rat skin epidermis **(22).**

3-Morphometric study:

Observations were gathered using a "Leica Qwin 500 C" image analyzer computer system Ltd. (Cambridge, England). The image analyzer was made out of "Leica Qwin 500 C" software, a colored video camera, a colored monitor, and an IBM personal computer hard drive attached to the microscope. The image analyzer was first automatically calibrated so that the measurement units (pixels) generated by the image analyzer programme were converted into real micrometer units. This study used 10 non-overlapping readings from each animal in different groups, which were calculated by two observers who were blind to the experimental group.

The following parameters were assessed: a) The epidermal thickness after 21 days b) The area percent of collagen fibers after 7 and 21 days c) The area percent of elastic fibers after 21 days d) The PCNA labeling index after 7 days.

Biochemical study:

At the end of the experiment, fresh tissue skin samples which were obtained from the wound and the surrounding 0.5cm normal tissue was kept frozen at -80 c° till it subjected to tissue analysis of the following parameters: a) The expression level of Nrf2 and Keap-1 b) proliferation related genes PI3K/Akt

c) Inflammatory markers (TNFα and IL-6) d) Transforming growth factor (TGFβ) and vascular endothelial growth factor (VEGF)

Statistical analysis:

Using the SPSS version 16.0 statistical program, the biochemical and morphometric data were statistically analyzed. Information presented as mean ± SE. Analysis of variance with one way (ANOVA) was used to evaluate comparisons between the groups. For statistical significance, a difference has to be $P < 0.05$ and $p \leq 0.01$ was considered highly significant.

Results

1- Histological Results of control group (normal skin):

Haematoxylin and Eosin (H&E) Stain, showing the upper surface is covered by epidermis. Many hair follicles and associated sebaceous glands were seen within the dermis; the hair follicles appear as downgrowth invaginations of the epidermis into

the dermis (Fig.4 A). **Masson's trichrome (MT) stain;** showing blue stained bundles of collagen fibers that form most of the thickness of dermis were detected (Fig.4 B). **Orcein- Stain** was showing thin dark brown elastic fibers in the dermis (Fig.4 C). **Anti-PCNA antibody – Stain,** demonstrating spread moderate to dense nuclear brown immunoreactive cells in the outer root sheath (ORS) of hair follicles and stratum Basale were observed (Fig.4 D).

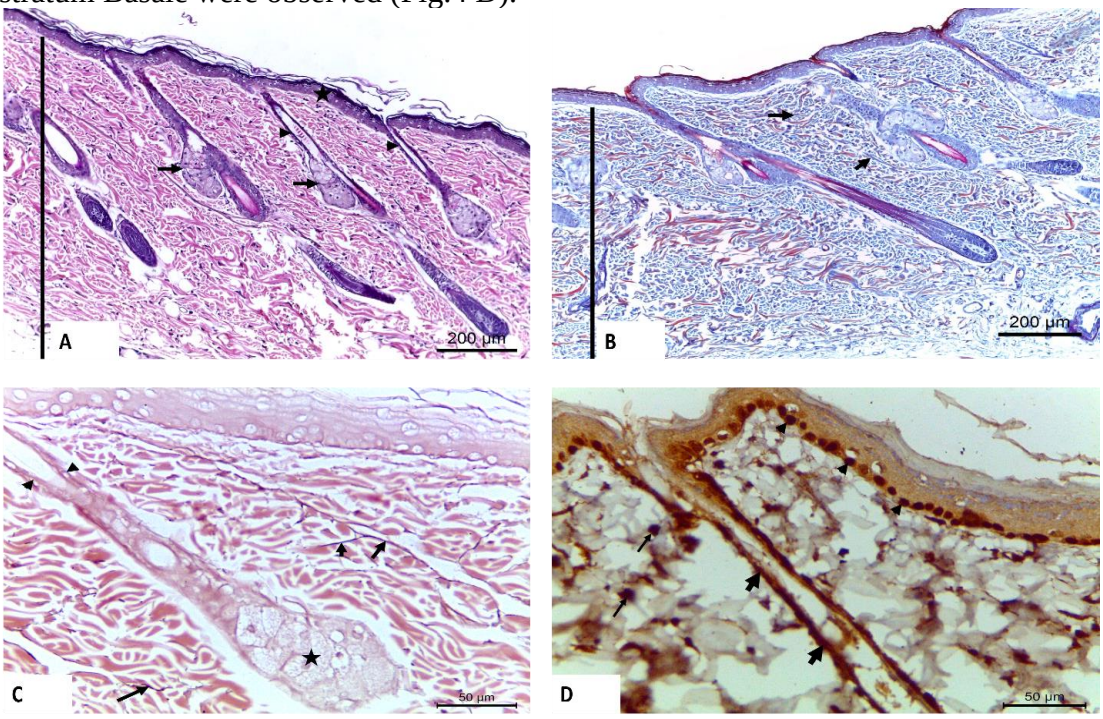

Fig. 4: skin stained sections of the control group I **A;** H& E stained section showed normal histological architecture of the skin consisting of epidermis (the black star). Many hair follicles (the black arrow head), the hair follicles invaginations into the dermis (the black line) and sebaceous glands (the black arrow) were seen within the dermis; **B;** Masson Trichrome stained section showing blue stained bundles of collagen fibers (the arrows) were seen. **C;** Orcein- Stained Section showing thin dark brown elastic fibers (the arrows) in the dermis mainly around sebaceous glands (the star) and hair follicles (the arrow head). **D;** Anti-PCNA antibody Stained showing nuclear brown immunoreactive cells in stratum Basale (the arrow heads) and cells of the outer root sheath (ORS) of hair follicles (the thick arrows). The immunoreactivity is also detected in the fibroblast cells (the thin arrows)**.**

2- Histopathological Results of group A:

Haematoxylin and Eosin-Stained (H&E) sections from Subgroup IIA (operated skin), the wound area showed an extensive absence of epidermis, loss of skin appendages, papillary dermis and most of the reticular dermis, wide spread of inflammatory cell infiltration (Fig.5 A). In subgroup IIIA (treated with MSCs) the wound defect was covered with crust and irregular thickness epidermis. The epidermis adjacent to the wound showed reactive proliferation (Fig.5 B). In subgroup IVA (treated with exosomes), the epidermis adjacent to the wound showed reactive enlargement of keratinocytes. The wound bed is filled with granulation tissue and marked inflammatory cell infiltrate (Fig.5 C). In subgroup VA (treated with PRP) the wound surface revealed failure of crust formation. The adjoining epidermis was thickened at the wound edge. The wound bed was filled with highly cellular granulation tissue (Fig.5 D).

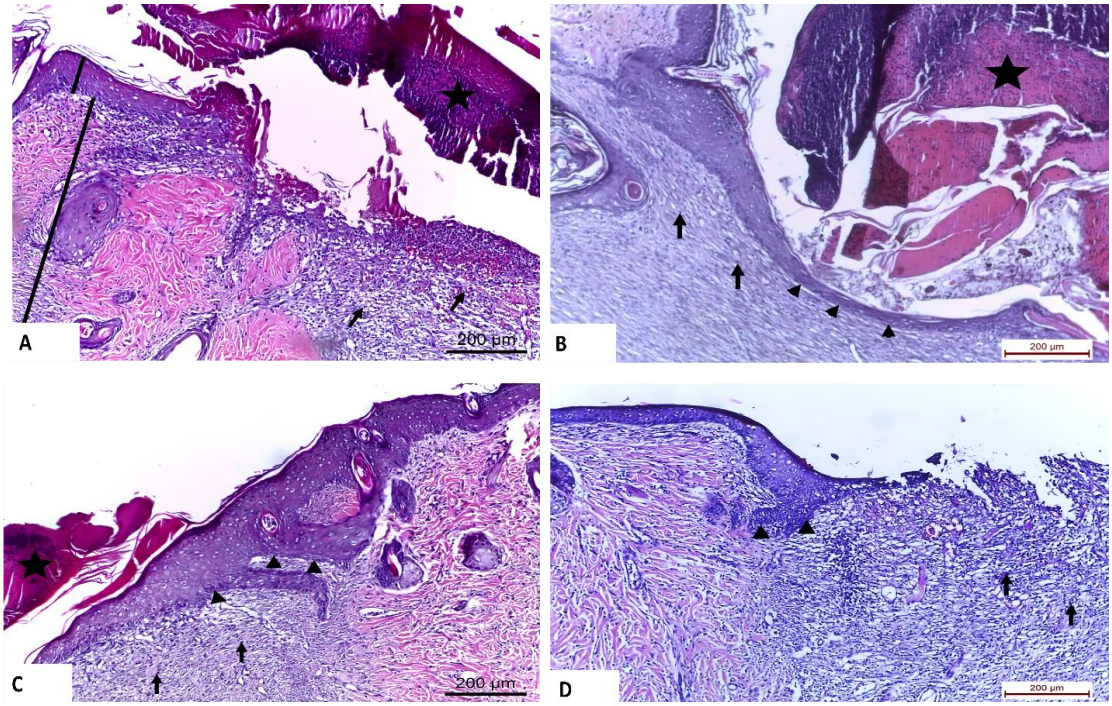

Fig. 5: H& E stained sections from group A. **A: section from** subgroup IIA revealed crust formation (the star). The wound site displayed total absence of epidermis, loss of skin appendages with inflammatory cell infiltrate (the arrows). **B: section from** subgroup IIIA the wound defect covered with crust (the star). The nearby epidermis showed reactive proliferation with irregular epidermal thickness (the arrow head). The underlying granulation tissues at the wound bed showed marked inflammatory infiltrate (the arrows). **C: section from** subgroup IVA the wound defect was covered by crust (the star) and filled with highly cellular granulation tissues (the arrows). The epidermis adjacent to the wound showed reactive enlargement of keratinocytes under the formed crust (the arrow head). **D: section from** subgroup VA the wound surface revealed failure of crust formation. The adjacent epidermis was seen thickened at the wound edge (the arrow head). The wound bed was filled with highly cellular granulation tissue (the arrows).

Masson's trichrome (MT) Stained Sections from subgroup IIA (operated skin) showing, sparse and haphazardly arranged collagen bundles in the regenerated part of the dermis (Fig.6 A). In subgroup IIIA (treated with MSCs) the wound bed showed prominently deposited thin collagen fibers within the regenerated granulation tissues (Fig.6 B). In subgroups IVA and VA (treated with exosomes and PRP, respectively) the wound bed showed prominent thin collagen fibers were deposited within the regenerated granulation tissues. At the edges of the wound and the nearby dermis thick collagen bundles were detected (Fig. 6 C&D).

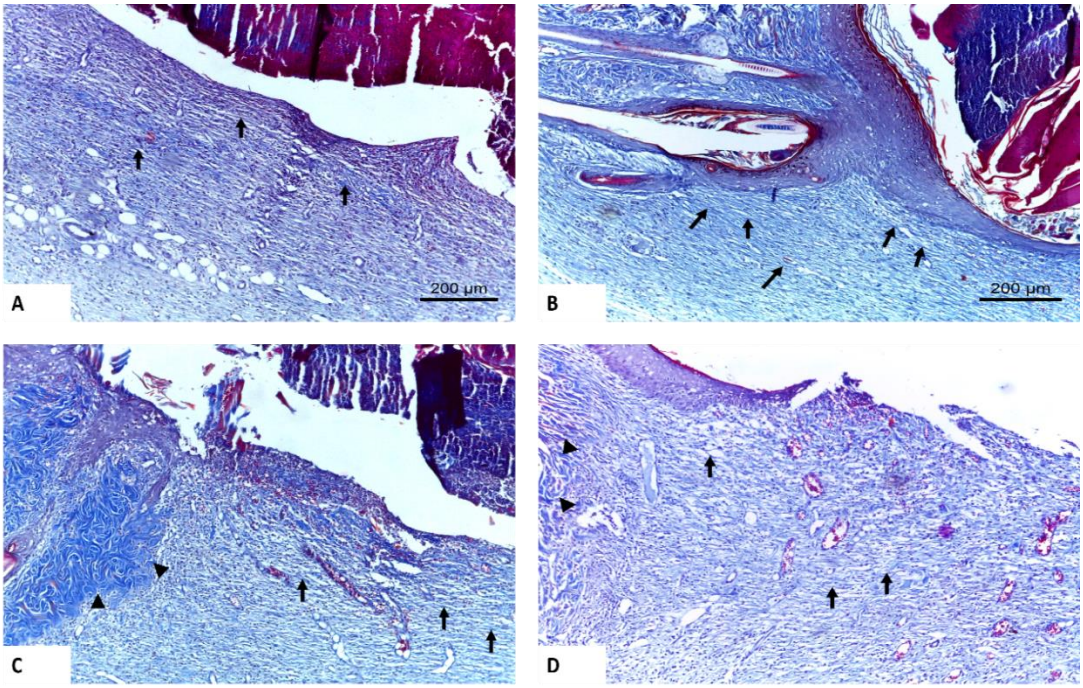

Fig. 6: Masson's trichrome (MT) stained sections of skin of rats of group A**. A: section from** subgroup IIA exhibiting sparse and haphazardly arranged blue collagen bundles (the arrows) in the regenerated part of the dermis. **B: section from** subgroup IIIA the wound bed demonstrated substantial deposition of thin light blue collagen fibers (the arrows) within the regenerated granulation tissues. **C: section from** subgroup IVA the wound bed clearly showed deposition of thin blue collagen fibers (the arrows) within the regenerated granulation tissues. Thick dark blue collagen bundles (the arrow head) were present at wound edges in the adjacent dermis. **D: section from** subgroup VA showed deposition of thin blue collagen fibers (the arrows) and thick dark blue collagen bundles (the arrow head) were present at wound edges.

Anti-PCNA antibody - Stained Sections from subgroup IIA (operated skin), showing moderate immunoreactive nuclei were detected in the fibroblastic cells only (Fig.7 A). Subgroups IIIA, IVA and VA (treated with MSCs, exosomes and PRP respectively) showing moderate to dense immunoreactive nuclei were detected in the cells of stratum basale and some cells stratum spinosum and in the fibroblastic cells (Fig.7 B,C and D respectively).

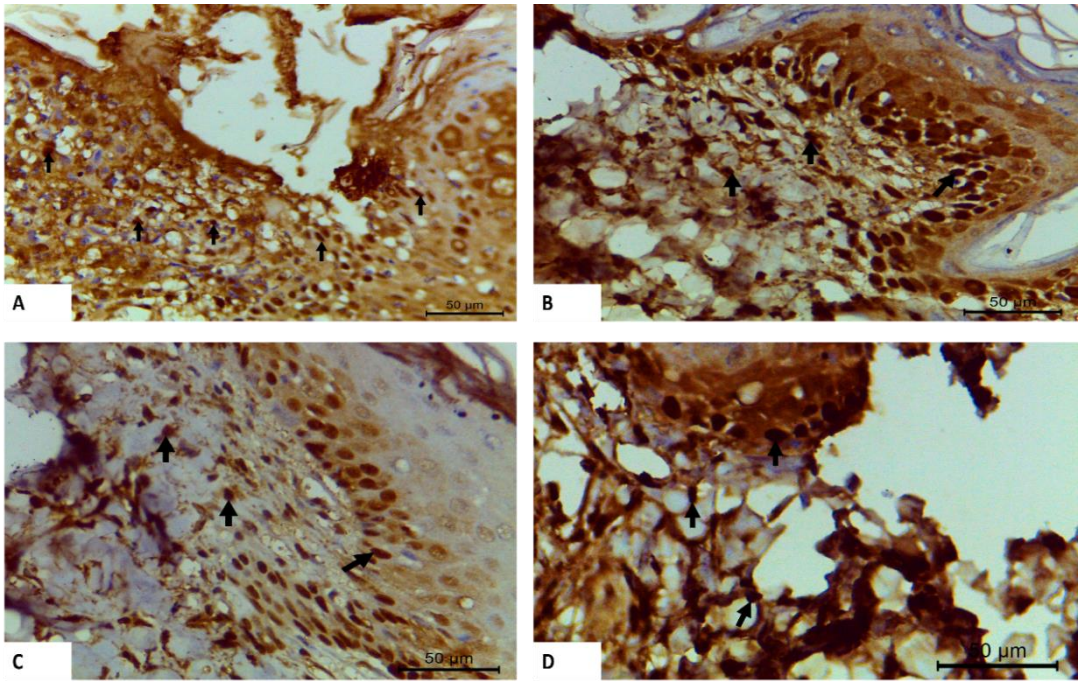

Fig.7: Anti-PCNA antibody Stained Sections of skin of rats of group A. **A: section from** subgroup IIA revealed moderate immunoreactive nuclei in the fibroblastic cells (the arrows). **B, C and D: sections from** subgroup IIIA, IVA and VA respectively showed moderate to dense immunoreactive nuclei in the cells of stratum basale, stratum spinosum and in the fibroblastic cells between the regenerated granulation tissue (the arrows).

3- Histopathological Results of group B:

Haematoxylin and Eosin-Stained (H&E) sections from Subgroup IIB (operated skin) revealed that the site of wound was completely covered with thin regenerated epidermis (Fig.8 A). In subgroup IIIB, IVB and VB, the wound site was shown full dermal and epidermal regeneration with fully retain of the skin appendage (Fig.8 B, C, and D respectively).

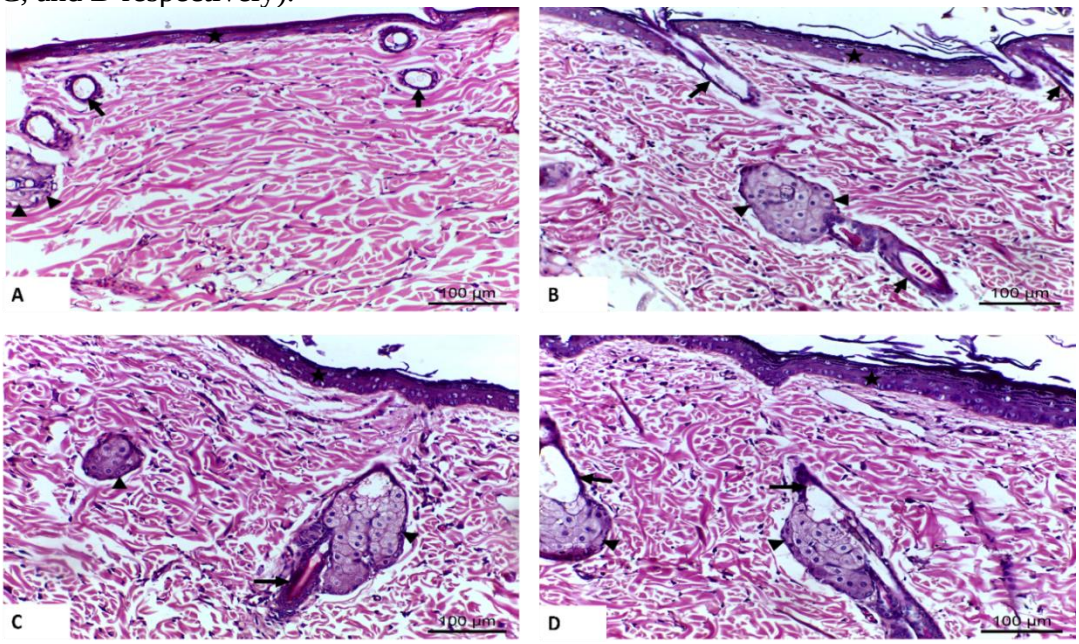

Fig. 8: H& E stained sections of skin of rats of group B. **A: section from** subgroup IIB revealed that the wound was completely covered with totally thin regenerated epidermis (the star). The underlying regenerated dermis exhibited hair follicles (the arrows) and sebaceous gland (the arrow head). **B, C and D: sections from** subgroups IIIA, IVA and VA

respectively, the wound area reveals completely regenerated and relatively thick epidermis (the stars). The hair follicles (the arrows) and the sebaceous glands (the arrows head) are detected within the regenerated dermis.

Masson's trichrome (MT) Stained Sections from subgroup IIB (operated skin) showed deposited collagen bundles aligned horizontally in one direction in the regenerated scar and occupied the whole thickness of the dermis (Fig.9 A). The sections in subgroups IIIB, IVB and VB were reveled thick dense collagen bundles distributed in various directions in a network like manner (Fig.9 B, C and D respectively).

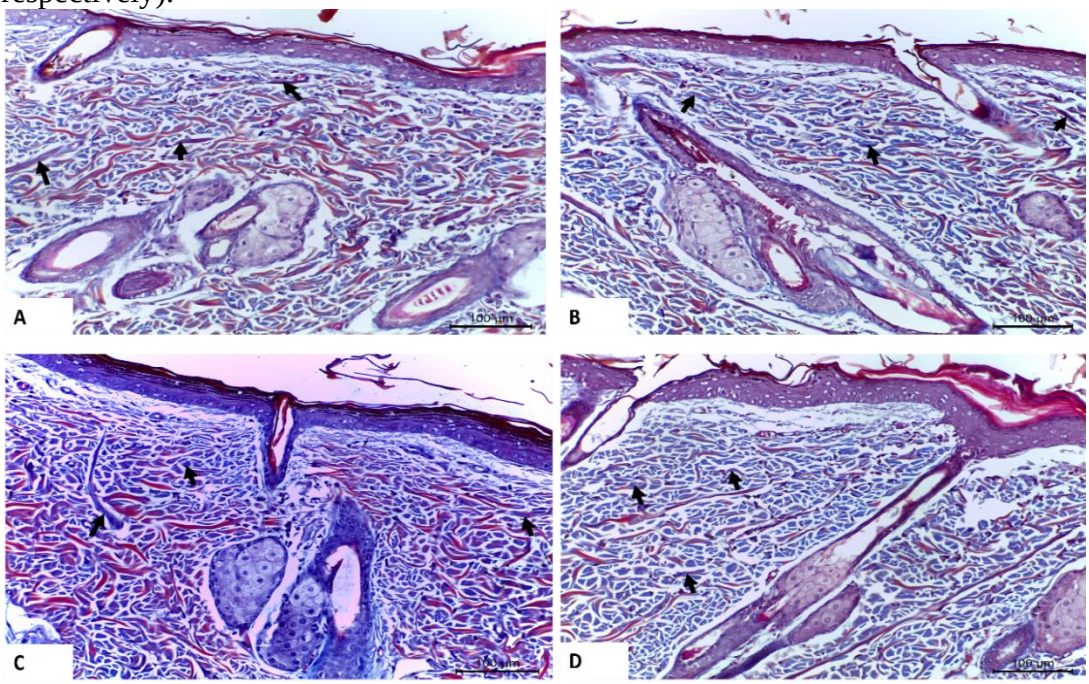

Fig. 9: Masson's trichrome (MT) stained sections of skin of rats of group B. **A: section from** subgroup IIB showed dense blue collagen bundles (the arrows) aligned horizontally in one direction in the regenerated scar and occupied the whole thickness of the dermis. **B: section from** subgroup IIIB showed dense thick collagen bundles (the arrows) arranged in different directions. **C: section from** subgroup IVB revealed dense thick collagen bundles (the arrows) arranged in network like manner. **D: section from** subgroup VB exhibited thick dense collagen bundles (the arrows) distributed in several directions in network like organization.

Orcein- Stained Sections from subgroup IIB (operated skin) showed little to moderate amount of thin brown elastic fibers in the regenerated dermis mainly near the hair follicles (Fig.10 A). The sections in subgroups IIIB, subgroup IVB and subgroup VB**,** showed widespread of thin dark brown branching elastic fibers in the regenerated dermis mainly near the hair follicles (Fig.10 B, C and D respectively).

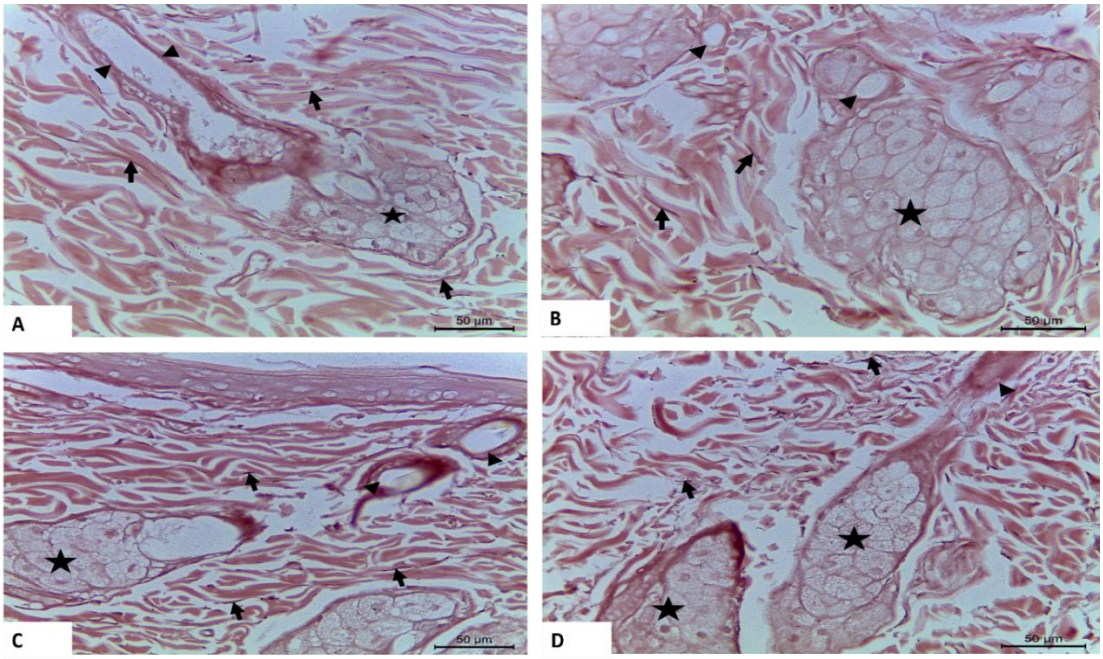

Fig 10: Orcein- Stained Sections of rats of group B. **A: section from** subgroup IIB showed little to moderate amount of thin brown elastic fibers (the arrows) in the regenerated dermis mainly near the hair follicles (the arrow head) and sebaceous glands (the star) . **B,C and D: sections from** subgroups IIIB, IVB and VB respectively, showed widespread of thin dark brown branching elastic fibers (the arrows) in the regenerated dermis mainly near the hair follicles (the arrows head) and sebaceous glands (the stars).

MORPHOMETRIC RESULTS

1-Morphometric results assessed in group A:

Area percent of collagen fibers

Comparing each group to the control group I revealed statistically significant differences. Additionally, there was statistically significant increase in collagen fibers (subgroup IIIA, subgroup IVA and subgroup VA) in compare with subgroup IIA ($p < 0.05$). Also both subgroup IIIA and subgroup VA exhibited a statistically significant increase when compared to subgroup IVA ($p < 0.05$). **(Table 1)**

Number of PCNA Immunopositive

There was statistically significant decrease in subgroup **IIA** ($p < 0.05$). However, there was significant increase in in immune positive cells in subgroups **IIIA** and **IVA** when compared to control group **I**. The difference between subgroup **VA** and group **I** was statistically non-significant ($P > 0.05$). However, there was statistically significant decrease in subgroup **VA** in compare with (subgroup **IIIA**, subgroup **IVA)** ($p < 0.05$). **(Table 1)**

Table 1: comparative quantitative histomorphometric analysis in group A

	Control	IA	III A	IV A	V A	P value
collagen area percentage	50.08± 0.80	15.47± 0.45 *	36.02± 0.86 *#	30± 1.45 *#$@	35.18± 1.99 *#	<0.001
PCNA Numbers	10.50± 1.87	6.33± 1.21 *	16.17± 1.17 *#	14± 0.89 *#	11.50± 1.05 #$@	<0.001

2- Morphometric results assessed in group B:

Epithelial thickness

There was no statistically significant difference between (subgroup III B and subgroup IVB) in compare with group I ($p > 0.05$), But there was statistically significant difference found between subgroup **II**B and subgroup V B when compared to group I ($p < 0.05$) and statistically significant difference was found between (subgroup IIIB and subgroup IVB) when compared to subgroup V B ($p < 0.05$). **(Table 2)**

Area percent of collagen fibers

There was statistically significant increase ($P < 0.05$) in the area percent of collagen fibers in all treated groups as compared with operated control groups. However, there was no statistically significant difference between the treated groups (subgroup III B and subgroup IVB and subgroup V B). **(Table 2)**

Area of elastic fibers

There was no statistically significant difference between the treated groups (subgroup IIIB and subgroup IVB and subgroup VB) and control group I ($p > 0.05$), but there was statistically significant decrease in subgroup IIB when compared to control group I and the treated groups ($p < 0.05$). **(Table 2)**

Table 2: comparative quantitative histomorphometric analysis in group B

	Control	IB	III B	IV B	V B	P value
epithelial thickness	49.95± 1.73	41.37± 1.77 *	47.57± 1.03 #	47.38± 0.70 *#	44.87± 1.24 *#$@	<0.001
collagen area percentage	50.08± 0.80	42.42± 1.92 *	47.80± 0.63 *#	45.97± 0.76 *#	46.82± 0.82 *#	<0.001
elastic fibers area percentage	19.67± 0.58	11.12± 0.50 *$@	18.60± 0.51 #	18.77± 0.71 #	19.03± 0.75 #	<0.001

Values are represented as mean ±SD

*: statistically significant compared to corresponding value in normal control group I (P<0.05)

#: statistically significant compared to corresponding value in MSC group III (P<0.05)

$: statistically significant compared to corresponding value in exosomes group IV (P<0.05)

@: statistically significant compared to corresponding value in PRP group V (P<0.05)

BIOCHEMICAL STUDY:

1- Nuclear factor-erythroid factor 2-related factor2 (Nrf2)

In group A, this finding shows significant increase ($p<0.001$) in groups treated with MSCs, exosomes or PRP (**IIIA, IVA** and **VA)** in compare with the operated control (**IIA).** Also, there was no significant difference between the treated groups with each other ($P > 0.05$). **(Table 3)**

In group B, this finding shows significant increase ($p<0.001$) in groups treated with either MSCs, exosomes or PRP (**III B, IVB** and **VB)** in compared with the operated control (**IIB)**, however no statistically significant difference between the MSCs treated group and the control group **I** ($P > 0.05$) but there was statistically significant decrease in the exosomes or PRP treated group (**IVB** and **VB)** in compare with the control group. No significant difference between the treated groups each other ($P > 0.05$). **(Table 4)**

2- Kelch-like ECH-associated protein 1(Keap-1)

In group A, this finding shows significant increase ($p<0.001$) in subgroups **IIA** (operated control) than the control group **I**, however no statistically significant

difference between the **IIIA** subgroup and the control group **I** (P > 0.05). But there was statistically significant increase in **IV**A or **VA** subgroups in compare with the control group **I** (p<0.001). **(Table 3)**

In group B, the finding shows significant decrease (p<0.001) in groups treated with either MSCs, exosomes or PRP (**IIIB, IVB** and **VB)** than the operated control **IIB**, however statistically no significant difference between the **IIIB** subgroup and the group **I** (P > 0.05) but there was statistically significant difference between the **IVB** or **VB** subgroups and group **I** (p<0.001). No significant difference between the treated groups each other (P > 0.05). **(Table 4)**

3- Phosphatidylinositol 3-kinase

In group A, this finding shows significant increase (p<0.001) in subgroups **IIIA** (MSCs) than **IIA**, however no statistically significant difference between the **IIIA** subgroup and group **I** (P > 0.05), but there was statistically significant difference between **IVA or VA** subgroups and group **I** (p<0.001). **(Table 3)**

In group B, this finding shows statistically significant increase (p<0.001) in subgroups **IIIB, IV**B and **VB** than the control group **I**, however no statistically significant difference between the treated groups each other (P > 0.05). But there was statistically significant difference between the treated groups and subgroup **IIB** (P < 0.001). **(Table 4)**

4- Ak strain transforming pathway

In group A, this finding shows significant increase (p<0.001) in subgroups **IIIA** than **IIA**, however statistically no significant difference between the subgroups **IIIA**, subgroup **VA** and group **I** (P > 0.05), but there was statistically significant difference between subgroup **IVA** and group **I** (p<0.001). **(Table 3)**

In group B, this finding shows significant increase (p<0.001) in treated subgroups **IIIB, IVB and VB** in compare with **IIB**, however no statistically significant difference between the subgroups **IIIB** and subgroup **VB** and group **I** (P > 0.05). But there was statistically significant decrease in the subgroup **IVB** in compare with control group. **(Table 4)**

Table 3: comparative biochemical parameters in group A

	normal skin	**Ia**	**III a**	**IV a**	**V a**	**P value**
Nrf2	1.03±0.02	0.35±0.15 *	0.78±0.06 #	0.62±0.04 *#	0.61±0.09 *#	< 0.001
Keap-1	1±0.01	5.13±0.8 *	2.41±0.6 #	3.14±0.32 *#	2.7±0.66 *#	< 0.001
PI3K	1.04±0.03	0.38±0.11 *	0.84±0.06 #	0.69±0.12 *	0.68±0.2 *	0.001
Akt pathway	1.03±0.01	0.41±0.07 *	0.78±0.1 #	0.61±0.12 *	0.71±0.18	0.001

Table 4: comparative biochemical parameters in group B

	normal skin	**Ib**	**III b**	**IV b**	**V b**	**P value**
Nrf2	1.03±0.02	0.23±0.09 *	0.83±0.05 #	0.62±0.13 *#	0.67±0.17 *#	< 0.001
Keap-1	1±0.01	6.17±1 *	1.68±0.33 #	2.8±0.21 *#	2.4±0.56 #	< 0.001
PI3K	1.04±0.03	0.19±0.04 *	0.87±0.09 *#	0.75±0.08 *#	0.74±0.02 *#	< 0.001
Akt pathway	1.03±0.01	0.3±0.05 *	0.81±0.15 #	0.76±0.07 *#	0.8±0.07 #	< 0.001

5&6- Vascular endothelial growth factor (VEGF) and Transforming growth factorβ (TGFβ)

Concerning VEGF in group B, it shows significant increase (p<0.001) in groups treated with either MSCs and exosomes (**IIIB, IVB)** than the operated control (**IIB),** however no statistically significant difference between the MSCs and exosomes

treated subgroups (**IIIB, IVB)** each other (P > 0.05). However, there was statistically significant difference between the treated subgroups and the control group. **(Table 5)**
Regarding TGFβ in group B, it shows statistically significant decrease (p<0.001) in subgroups **IVB** and **IIIB** than the subgroup **IIB**, there was statistically significant difference between the treated groups each other (P<0.05) in the favor of **IVB.** However, there was statistically significant difference between the treated groups and the control group**. (Table 5)**

7&8-Tumor necrosis factor α (TNFα) and Interleukin-6 (IL-6)
Concerning TNFα in group B, it shows statistically significant decrease (p<0.001) in subgroups **IV**B and **IIIB** than the subgroup **IIB**, however no statistically significant difference between the treated groups each other (P > 0.05). Additionally, there was no statistically significant difference between subgroup **VB** and subgroup **IIB** (P > 0.05). **(Table 5)**
Regarding IL-6 in group B, it shows statistically significant decrease in subgroups **IVB, IIIB** and subgroup **VB** than the subgroup **IIB**, there was statistically significant difference between the treated groups each other (P<0.05)in the favor of **IVB (Table 5)**.
Table 5: comparative biochemical parameters in group B

	normal skin	**Ib**	**III b**	**IV b**	**V b**	**Mean**
TNFα (pg/mg tissue)	574.49±20.11	1200.05±244.43 *	815.04±56.5 #	698.15±66.23 #	914.16±18.85	0.001
IL-6 (pg/mg tissue)	211.94±25.47	431.3±18.6 *	336.84±8.26 *#	239.59±15.04 #$	376.5±19.03 *#@	< 0.001
TGFβ (pg/mg tissue)	323.32±35.7	998.19±58.51 *	656.13±28.21 *#	510.98±64.15 *#	825.88±95.39 *@	< 0.001
VEGF (pg/mg tissue)	1166.01±152.07	355.83±40.13 *	823.83±22.61 *#	1032.32±83.55 #	541±52.04 *$@	< 0.001

Values are represented as mean ±SD
*: statistically significant compared to corresponding value in **normal skin** group (P<0.05)
#: statistically significant compared to corresponding value in Operative control group (P<0.05)
$: statistically significant compared to corresponding value in MSC group (P<0.05)
@: statistically significant compared to corresponding value in exosomes group (P<0.05)

Discussion
The process of wound healing is a complex process that is important to maintain the barrier function of skin **(23).** Four overlapping stages may be employed to describe skin regeneration: hemostatic, inflammatory, angiogenesis, proliferation. The onset of neoangiogenesis is an important phase in tissue regeneration and wound healing **(24)**.
The current work indicating that MSC, exosomes and PRP can mitigate the inflammatory response brought on by a variety of stressors by reducing the production of cytokines and chemokines, particularly in the exosomes-treated group, such as interleukin (IL-6) and tumor necrosis factor (TNF).
Our findings elaborated that treatment with MSC, exosomes, and PRP could enhance the expression of molecules linked to angiogenesis and the amount of VEGF, particularly in the exosomes-treated group. The outcomes additionally shown that MSC, exosomes, and PRP were accelerated the wound healing, improved re-epithelialization, and increased PCNA expression, particularly in the MSCs treated group.

The extracellular matrix (ECM) remodeling process typically lasts two weeks to over a year. The formation of the ECM and its reorganization is a crucial in determining the scarring extent. Collagen production and degradation are crucial for ECM reconstruction. The present findings indicate better collagen organization in the treated groups which is one of the potential mechanisms of reducing scar formation.

In the current study, BM-MSCs, extracellular vesicles (exosomes produced from stem cells), and PRP treated groups all showed enhanced neo-epithelial thickness. One of the crucial processes in the healing of skin wounds is re-epithelialization.

Furthermore, the present work evaluated the proliferation of neoepidermal tissue by Immunohistochemical staining of PCNA, positive cells were found in the basal layer in the normal skin; however, they were found throughout the dermis as well as the basal layer in the proliferating conditions.

The present study showed that BM-MSCs, extracellular and PRP treatment markedly increased the proliferation with a significant difference comparable to the control group. This finding was matching with **Isackson et al. (2012) (25)** who found that BMSCs- treated wounds exhibited significantly increased re-epithelialization, cellularity, and angiogenesis in mice. Also this finding is coincident with **Zhang et al., 2015(1)** who reported that the results of PCNA immunochemical staining showed that human umbilical cord MSC-derived exosomes and its derived exosomes groups had more PCNA-positive cells in wound area than that in control at the 7^{th} day. The previous findings were also in line with **Li et al., (2019) (26)** who concluded that exosomes improved of epithelization through their anti-inflammatory effects as they inhibit the secretion of proinflammatory enzymes and cytokines in diabetic rats.

Xu et al., (2020) (27) reported that PRP might considerably improve the re-epithelialization of wounds. They proposed that PRP could stimulate the production of several factors by tissue cells, including VEGF and TGF. The same outcome was obtained in the current study.

The present work showed that BM-MSCs, exosomes and PRP may promote the efficient increase in neovascularization around the wound site and VEGF release in the wound tissue. According **to Xu et al. (2020) (27)** and **Li and Wu (2022) (28)** PRP and exosomes can promote angiogenesis after trauma and burn by boosting endothelial cell growth and VEGF expression. Another mechanism for enhancing angiogenesis was suggested by **Ding et al.,2019 (29)** who found that the exosomes-mediated angiogenesis mechanism is thought to involve direct interaction between exosomes and the cells that would receive them in order to transport specific mRNAs and proteins from the exosomes origin. However, **Lee et al., (2013) (30)** predicted that exosomes down-regulating VEGF expression in breast cancer cells which suppress angiogenesis; this may be explained by another pathophysiology.

In addition, an experimental study on rabbits conducted by **Ostvar et al., 2015 (31)** in which PRP was applied to the lesions created on the backs of animals. The authors reported that re-epithelialization and collagen deposition were statistically significantly higher in treated groups comparable to the healthy control. In another hand, a study by **Abegao et al.2015 (32)** which obtained PRP from dogs to be topically applied on the wound sites created on rabbits, there was no significant difference between the treated groups regard to re-epithelialization and collagen deposition between the treated group and control group, this could be explained by using a PRP of different method of induction and experimental animal species.

In the current investigation, Masson's trichrome-stained skin sections demonstrated that after one week, the non-treated group (operated control) displayed haphazardly ordered collagen bundles deposition. After three weeks, collagen had horizontally

aligned in one direction with a homogeneous intercellular material, and collagen remodeling had failed. After one week, analysis of skin samples from the BM-MSCs, exosomes, and PRP treated groups demonstrated early deposition of thin collagen fibers.

Properly deposited and organized Collagen fibers in the wound minimize the probability of scar healing, which is good for enhancing the effectiveness of tissue remodeling **(33).**

After 3 weeks, the treated groups displayed remodeling and arrangement of thick dense collagen fibers in various directions in a network-like manner. This outcome is in corresponds with **Hu et al.,2019 (33)** who mentioned that MSC and MSC-exosomes can boost the synthesis of type I collagen, type III collagen, and elastin proteins, as well as enhancing the expression of their mRNAs levels. The prior authors added that exosomes enter the cell and transport their proteins and RNAs, into the recipient cells such as dermal fibroblast to regulate their proliferation and migration, which contribute to the synthesis of collagen and the growth of granulation tissue, both of which give structural support for the healing of wounds. Therefore, exosomes have significantly sped up the healing rate and minimize the scar width **(34).**

Regarding the previous results, **Zhou et al., 2021(24)** reported increased collagen maturity by Masson trichrome stain in exosomes treated group in comparison with the other groups. In the wound area, collagen maturity was more pronounced and the collagens I to collagen III ratios were lowered.

Xu et al., 2020 (27) have demonstrated that PRP usage promotes collagen deposition and significantly reduces healing time. By measuring α-SMA, which is particularly expressed by myofibroblasts, the authors concluded that greater quantities of myofibroblasts were present at the wound area following PRP treatment for wound healing.

The current research showed a statistically significant increase in elastic fibers area percentage in all treated groups comparable to the operated control group. No significant between the treated groups and the control skin nor between them each other. **Ismail & Aboulkhair, 2018 (35)** reported the same result by intravenous injection of exosomes in rats with wound size (1.5 x 1.5 cm). **Ochiai et al., 2017 (36)** also have reported increasing in elastic fibers formation when they transplant mesenchymal stem cells in acute cutaneous wounds of pigs.

Regards to NRF2 gene, there was statistically significant difference between the BM-MSCs, exosomes and PRP treated groups (particularly the MSCs) compared to the operated control for NRF2 gene expression favoring the treated groups. This finding is in line with **Wang et al., 2020 (37)** who established that the antioxidant capacities of MSC and exosomes are regulated by the NRF2 defense system.

Due to the fact that Nrf2 is extremely sensitive to oxidative stress, pretreatment with an NRF2 activator lowered the degree of oxidative stress in wounds and accelerated wound healing. This is because it targets the inflammation and proliferation phases of wound healing **(38).**

Regarding PI3K/AKT the current study showed that BM-MSCs significantly counteracted wound induced-stress which cause reduction in phosphorylation of PI3K/AKT expression levels in wound tissue cells that promotes the fibroblast proliferation. This finding is consistent with **Zhang et al., 2018 (39) and Li et al., 2019(26),** who showed that MSCs and Exosomes can speed up collagen synthesis and deposition by enhancing fibroblast migration and proliferation through the PI3K/Akt signaling pathway. This outcome implies that the therapeutic effects of BM-MSCs

and exosomes on the damaged wound healing in skin cells could involve activations of PI3K/AKT signaling pathways.

Regarding TNFα Level, there was significantly decrease in the MSCs or exosomes groups than in the PRP group. While there was a significant decrease in all treated groups when compared to the operated control group, there was still a significant increase when compared to normal levels. The groups treated with MSCs and exosomes had the best results for this criterion. This result is in line with **Liu et al. (2014) (40), Lee et al. (2016)(41), and Gad et al. 2020(42).**

Gad. et al., 2020 (42) observed that topical treatment of PRP sped up the healing of wounds in a rat model; treated animals showed lower levels of corticosterone and inflammatory cytokines, such as IL-1, IL-6, and TNFα, on day 14 compared to day 7 of wound induction. They hypothesized that the increased concentrations of anti-inflammatories that have the ability to reduce inflammatory biomarkers and proinflammatory cytokines may be to blame for this finding.

The present study showed that, MSCs, exosomes and PRP treatment may significantly decrease the gene expression of IL-6 in wound tissues in 21th day especially the exosomes. This suggested that MSCs, Exosomes and PRP has a capability to control wound inflammation, assisting in the enhancement of skin wound healing, according to **Liu et al. (2014)(40) and Gad et al. (2020)(42).**

Johnson et al., 2020 (43) reported that IL-6 is an inflammatory mediator, plays a vital role in the precise healing of cutaneous wounds by affecting dermal fibroblast migration and stimulates keratinocyte migration and proliferation.

After 21 days, the exosomes and MSCs groups showed significantly decreased in TGF-β levels when compared to the operated control group, according to the current study. This is consistent with **Jiang et al 2020(44),** who suggested that BM-MSC and exosomes efficiently improve cutaneous wound healing by blocking the TGF-β pathway. Moreover, **Zhang et al., 2021 (45)** shown that MSCs have an ability to release exosomes to promote regenerative wound repair. Exosomes produced by MSCs disrupt the TGF-β signaling pathway and reduce the development of myofibroblasts. They view this discovery as a potential substitute for cell therapy, which may be an innovative way to stop scar formation during wound healing in clinic.

Regarding the effect of PRP, the present work showed up regulation TGF-β in the PRP treated group than the MSCs or exosomes. This finding supported by **Nurden et al., 2008 (46)** who reported that platelets have a great impact in regulating the process of wound healing in the treatment of burns by releasing growth factors include TGF-β.

References

1. **Zhang, B., Wang, M. and Gong, A et al., (2015).** Huc MSC-exosomes mediated-Wnt4 signaling is required for cutaneous wound healing. Stem cells, 33(7), 2158-2168 doi: 10.1002/stem.1771.
2. **Maxson, S., Lopez, E. A. & Yoo, D. et al., (2012).** Concise review: role of mesenchymal stem cells in wound repair. Stem cells translational medicine, 1(2), 142-149 doi: 10.5966/sctm.2011-0018.
3. **Augello, A., Kurth, T. B. and De Bari, C. (2010).** Mesenchymal stem cells: a perspective from in vitro cultures to in vivo migration and niches. Eur. Cell Mater, 20(121), 33 doi: 10.22203/ecm.v020a11.
4. **Silva JD, Lopes-Pacheco M and Paz AHR et al.** (2018) Mesenchymal stem cells from bone marrow, adipose tissue, and lung tissue differentially mitigate lung and

distal organ damage in experimental acute respiratory distress syndrome. Crit. Care Med 46: e132-e140 doi: 10.1097/CCM.0000000000002833.

5. **Phinney, D. G., and Prockop, D. J. (2007).** Concise review: mesenchymal stem/multipotent stromal cells: the state of transdifferentiation and modes of tissue repair current views. Stem cells, 25(11), 2896-2902 doi: 10.1634/stemcells.2007-0637.
6. **Lazarus, H. M., Koc, O. N. and Devine, S. M et al., (2005).** Cotransplantation of HLA-identical sibling culture-expanded mesenchymal stem cells and hematopoietic stem cells in hematologic malignancy patients. Biology of blood and marrow transplantation, *11*(5), 389-398 doi: 10.1016/j.bbmt.2005.02.001.
7. **Nikolidakis D and Jansen JA (2008).** The biology of platelet-rich plasma and its application in oral surgery: literature review. Tissue Eng. Part B Rev.; 14:249–258 doi: 10.1089/ten.teb.2008.0062.
8. **Crovetti G, Martinelli G and Issi M et al., (2004).** Platelet gel for healing cutaneous chronic wounds. Transfus. Apher. Sci., 30:145–151 doi: 10.1016/j.transci.2004.01.004.
9. **Yamada Y, Ueda M and Naiki T et al., (2004).** Autogenous injectable bone for regeneration with mesenchymal stem cells and platelet-rich plasma: tissue-engineered bone regeneration. Tissue Eng.; 10:955–964 doi: 10.1089/1076327041348284.
10. **Zou, X., Gu, D. and Xing, X. et al., (2016).** Human mesenchymal stromal cell-derived extracellular vesicles alleviate renal ischemic reperfusion injury and enhance angiogenesis in rats. American Journal of Translational Research, 8(10), 4289-4299
11. **Camussi, G., Deregibus, M.C. and Bruno et al., (2010).** Exosomes/microvesicles as a mechanism of cell-to-cell communication. Kidney International, 78(9), 838-848 doi: 10.1038/ki.2010.278.
12. **Qiu, G., Zheng, G. and Ge, M. et al., (2018).** Mesenchymal stem cell-derived extracellular vesicles affect disease outcomes via transfer of microRNAs. Stem Cell Research and Therapy, 9(1), 320 doi: 10.1186/s13287-018-1069-9.
13. **Bruno, S., Grange, C. and Deregibus, M., et al. (2009).** Mesenchymal stem cell-derived microvesicles protect against acute tubular injury. Journal of the American Society of Nephrology, 20(5): 1053-1067. Doi: 10.1681/ASN.2008070798.
14. **Sonnleitner D, Huemer P and Sullivan DY, (2000)** A simplified technique for producing Platelet-rich plasma and Platelet Concentrate for intraoral bone grafting techniques: A technical note. Int. J Oral Maxillofac. Implants; 15:879-882.
15. **Hashem, H., Mobasher, M. O. and Mohamed, M., et al. (2018).** Efficiency of Adipose-Derived versus Bone Marrow-Derived Stem Cells in Modulation of Histopathological Changes and CD31 Immunoexpression during Wound Healing in Rats. Journal of Biochemistry & Cell Biology: 1-9.
16. **Rodriguez, J., Boucher, F. and Lequeux, C. et al. (2015).** Intradermal injection of human adipose-derived stem cells accelerates skin wound healing in nude mice. Stem cell research & therapy, 6(1): 241 doi: 10.1186/s13287-015-0238-3 .
17. **Tatar, C., Aydin, H. and Karsidag, T. et al. (2017).** The effects of platelet-rich plasma on wound healing in rats. Int. J Clin. Exp. Med, 10(5), 55-70.
18. **Basiouny, H., Salama, N. and El Maadawi et al. (2013).** Effect of bone marrow derived mesenchymal stem cells on healing of induced full-thickness skin wounds in albino rat. International journal of stem cells, 6(1): 12 doi: 10.15283/ijsc.2013.6.1.12.

19. **Bancroft J and Gamble M (2008).** Theory and Practice of Histological Techniques., staining methods, Churchill Livingstone, Edinburgh, London, Madrid, Melbourne, New York and Tokyo,7: 121-135 and 263 -325.
20. **Kiernan JA (2001).** Histological and histochemical methods: theory and practice, 3: 111-162.
21. **Suvarna SK, Layton C and Bancroft JD (2012):** Bancroft's theory and practice of histological techniques, Elsevier Health sciences, Churchill, Livingstone, 7: 215- 239.
22. **Ghannam, S., Korayem, H. and Farghaly et al. (2018).** The effect of chitosan nanosilver dressing versus mesenchymal stem cells on wound healing. Journal of African Association of Physiological Sciences, 6(1):23-31.
23. **Han, G., & Ceilley, R. (2017).** Chronic wound healing: a review of current management and treatments. Advances in therapy, 34, 599-610 doi: 10.1007/s12325-017-0478-y.
24. **Zhou, Y., Zhao, B. and Zhang, X. L et al., (2021).** Combined topical and systemic administration with human adipose-derived mesenchymal stem cells (hADSC) and hADSC-derived exosomes markedly promoted cutaneous wound healing and regeneration. Stem cell research & therapy, 12(1), 1-12 doi: 10.1186/s13287-021-02287-9.
25. **Isackson D., Cook K. and McGill L. et al. (2012):** Mesenchymal stem cells increase collagen infiltration and improve wound healing response to porous titanium percutaneous implants. Med Eng. Phys. 35 (6), 743-753 doi: 10.1016/j.medengphy.2012.08.002.
26. **Li, M., Wang, T. and Tian, H., et al. (2019).** Macrophage-derived exosomes accelerate wound healing through their anti-inflammation effects in a diabetic rat model. Artificial Cells, Nanomedicine, and Biotechnology, 47(1), 3793-3803 doi: 10.1080/21691401.2019.1669617.
27. **Xu, P., Wu, Y. and Zhou, L., et al., (2020).** Platelet-rich plasma accelerates skin wound healing by promoting re-epithelialization. Burns & trauma, 8:1-4 doi: 10.1093/burnst/tkaa028.
28. **Li, D., and Wu, N. (2022).** Mechanism and application of exosomes in the wound healing process in diabetes mellitus. Diabetes Research and Clinical Practice, 10 (9):882 doi: 10.1016/j.diabres.2022.109882.
29. **Ding, J., Wang, X. and Chen, B., et al. (2019).** Exosomes derived from human bone marrow mesenchymal stem cells stimulated by deferoxamine accelerate cutaneous wound healing by promoting angiogenesis. BioMed. Research international, 5(11)1-16 doi: 10.1155/2019/9742765.
30. **Lee, J. K., Park, S. R. and Jung, B. et al, (2013).** Exosomes derived from mesenchymal stem cells suppress angiogenesis by down-regulating VEGF expression in breast cancer cells. PloS one, 8(12), 4256 doi: 10.1371/journal.pone. 0084256..
31. **Ostvar O, Shadvar S and Yahaghi E., et al. (2015).** Effect of platelet-rich plasma on the healing of cutaneous defects exposed to acute to chronic wounds: a clinico-histopathologic study in rabbits. Diagn. Pathol; 10: 85-90 doi: 10.1186/s13000-015-0327-8.
32. **Abegão K, Bracale B and Delfim I, et al. (2015).** Effects of heterologous platelet-rich plasma gel on standardized dermal wound healing in rabbits. Acta. Cir Bras; 30: 209-215 doi: 10.1590/S0102-865020150030000008.

33. **Hu, P., Yang, Q. and Wang, Q., et al. (2019).** Mesenchymal stromal cells-exosomes: a promising cell-free therapeutic tool for wound healing and cutaneous regeneration. Burns & trauma, 7,1-14 doi: 10.1186/s41038-019-0178-8.
34. **Guo, S. C., Tao, S. C. and Yin, W. J. et al., (2017).** Exosomes derived from platelet-rich plasma promote the re-epithelization of chronic cutaneous wounds via activation of YAP in a diabetic rat model. Theranostics, 7(1), 81 doi: 10.7150/thno.16803.
35. **Ismail, D., and Aboulkhair, A. (2018).** Histological evaluation of the emerging role of adipose stem cells-derived exosomes in cutaneous wound healing in albino rats. Egyptian Journal of Histology, 41(4), 459-472.
36. **Ochiai, H., Kishi, K., Kubota, Y., et al., (2017).** Transplanted mesenchymal stem cells are effective for skin regeneration in acute cutaneous wounds of pigs. Regenerative Therapy, 7, 8-16 doi: 10.1016/j.reth.2017.06.003.
37. **Wang, T., Jian, Z. and Baskys, A., et al. (2020).** MSC-derived exosomes protect against oxidative stress-induced skin injury via adaptive regulation of the NRF2 defense system. Biomaterials, 257, 120264 doi: 10.1089/ten.teb.2008.0062.
38. **Liu, Y., Yang, X. and Liu, Y et al., (2021).** NRF2 signaling pathway: new insights and progress in the field of wound healing. Journal of Cellular and Molecular Medicine, 25(13), 5857-5868 doi: 10.1111/jcmm.16597.
39. **Zhang, W., Bai, X. and Zhao, B., et al. (2018).** Cell-free therapy based on adipose tissue stem cell-derived exosomes promotes wound healing via the PI3K/Akt signaling pathway. Experimental cell research, 370(2), 333-342 doi: 10.1016/j.yexcr.2018.06.035.
40. **Liu, L., Yu, Y. and Hou, Y et al., (2014).** Human umbilical cord mesenchymal stem cells transplantation promotes cutaneous wound healing of severe burned rats. PloS one, 9(2), e88348 doi: 10.1371/journal.pone.0088348.
41. **Lee D, Ayoub N, and Agrawal D (2016):** Mesenchymal stem cells and cutaneous wound healing: novel methods to increase cell delivery and therapeutic efficacy. *Stem Cell Res Ther*; 7: 37 doi: 10.1186/s13287-016-0303-6.
42. **Gad, S. B., Hafez, M. H., and El-Sayed, Y. S. (2020).** Platelet-rich plasma and/or sildenafil topical applications accelerate and better repair wound healing in rats through regulation of proinflammatory cytokines and collagen/TGF-β1 pathway. Environmental Science and Pollution Research, 27(32), 40757-40768 doi: 10.1007/s11356-020-10042-5. Epub 2020 Jul 15.
43. **Johnson, B. Z., Stevenson, A. W. and Prêle, C et al., (2020).** The role of IL-6 in skin fibrosis and cutaneous wound healing. Biomedicines, 8(5), 101 doi: 10.3390/biomedicines8050101.
44. **Jiang, T., Wang, Z., and Sun, J. (2020).** Human bone marrow mesenchymal stem cell-derived exosomes stimulate cutaneous wound healing mediates through TGF-β/Smad signaling pathway. Stem cell research & therapy, 11(1), 1-10 doi: 10.1186/s13287-020-01723-6.
45. **Zhang, Y., Pan, Y., and Liu et al., (2021).** Exosomes derived from human umbilical cord blood mesenchymal stem cells stimulate regenerative wound healing via transforming growth factor-β receptor inhibition. Stem cell research & therapy, 12(1), 1-14 doi: 10.1186/s13287-021-02517-0.
46. **Nurden, A. T., Nurden, P. and Sanchez, M et al., (2008).** Platelets and wound healing. Frontiers in Bioscience-Landmark, 13(9), 3532-3548 doi: 10.2741/2947.